CORRELATION OF THE MULTIPHASE FLOW COEFFICIENTS OF POROUS MEDIA WITH WETTABILITY: A PORE NETWORK APPROACH

CHRISTOS D. TSAKIROGLOU

Institute of Chemical Engineering and High Temperature Chemical Processes – Foundation for Research and Technology, Stadiou str., Platani, P.O.Box 1414, GR-26504 Patras, Greece

ABSTRACT

A pore-and-throat network including fractal-like roughness features along its surface is employed to simulate primary drainage and secondary imbibition by accounting for the quasistatic motion of menisci in pores and throats and varying the contact angle from 0^o (strongly water-wet conditions) to 180^o (strongly oil-wet conditions). The angle of sharpness of roughness features defines a range of contact angles within which the cross-section of the throat or pore is occupied completely by the one fluid and conditions of intermediate wettability are established. In contrast, outside this range, both fluids may coexist in a pore or throat. Such differences on the fluid distribution at the pore level affect strongly the capillary, electrical and hydraulic properties of the porous medium and are reflected in the capillary pressure, resistivity index, and relative permeability curves. The simulator is used to calculate the aforementioned two-phase flow coefficients as the pore system transits from strongly water-wet or strongly oil-wet to intermediate-wet conditions.

1. INTRODUCTION

The wettability of porous media plays an important role in a variety of multiphase flow processes of industrial and environmental interest: the enhanced oil and gas recovery from reservoirs rocks; the contamination of the unsaturated and saturated zones of the subsurface by industrial wastes, landfill leachates, pesticides, etc, and the implementation of remediation technologies; the CO_2 storage in depleted reservoirs of hydrocarbons and deep saline aquifers for reducing the greenhouse gas effects. In industrial practice, the wettability of porous rocks is usually quantified by calculating the wettability indices which are obtained through the proper integration of capillary pressure curves (USBM methods, see for details Anderson, 1986a,b). Given that, the capillary pressure curves depend on the interaction of the pore structure, the wettability and the saturation history (Morrow, 1976, 1990), any effort for the interpretation of experimental data of relative permeability functions and resistivity index is inevitably associated with the analysis of the corresponding capillary pressure curves.

Many efforts have been done to predict the macroscopic transport coefficients of reservoir rocks using pore network models. An extended review of the majority of these models is given by Sahimi (1995).Theoretical simulations of the drainage / imbibition cycles in non-circular pores have described the creation of mixed-wet conditions by taking into account the disjoining pressure and the stability of the thin wetting films surrounding the rock grains (Kovscek et al., 1993). Numerous models and theoretical simulators have been

developed to interpret the dependence of the two- and three-phase flow coefficients of porous media on the fractional / mixed wettability (Bradford et al., 1997; Hazlet et al., 1998; Blunt, 1998; Tsakiroglou and Fleury, 1999; Man and Jing, 1999; Laroche et al., 1999; Dicarlo, 2000; van Dijke et al., 2001; Jackson et al. 2003). Nevertheless, no mechanistic model has ever been suggested to quantify the experimentally observed (Anderson, 1986a,b) non-linear variation of the two-phase flow coefficients as a strongly water-wet or oil-wet pore system becomes intermediate-wet.

In the present work, a pore-and-throat network incorporating fractal-like roughness features along the pore walls is used to simulate the pressure-controlled primary drainage and secondary imbibition in porous media. The simulator is used to examine how the capillary pressure curve, the resistivity index and the water and oil relative permeability functions change as the contact angle is scanned from 0^o to 180^o, by placing emphasis on the contact angle range (60^o-120^o) of intermediate wettability.

2. PORE NETWORK MODEL

The pore space is modeled as a three-dimensional network of "spherical" pores interconnected through "cylindrical" throats (primary porosity) with roughness features (secondary porosity) superposed on the free surface of pores and throats (Tsakiroglou and Payatakes, 1993). The pore-diameter distribution (PSD), the throat-diameter distribution (TSD), and the primary porosity, ε_p, are used as input parameters for the construction of the primary network, whereas the pore-wall roughness is modeled as a fractal-like surface (as it is described below) by using as parameters the total porosity ε_t, the number of layers of roughness features, i_p, and the ratio of the surface area of the secondary pores to that of the primary pores, r_A. Two opposite sides of the network serve as entrance and exit whereas periodicity is imposed on the rest boundary throats surrounding the network.

2.1 Fractal roughness model

For the cylindrical axisymmetric throats we consider that their rough surface is formed by superposing successive layers of triangular prisms touching each other. For the spherical pores it is assumed that their surface is covered by successive layers of right circular cones arranged on a closed packing layer. The parameters of the model are: (1) the number of rough features per linear dimension of a roughness feature of the previous layer, n_r; (2) the number of layers of roughness features, i_p; (3) the common angle of sharpness of roughness features, w. It is worth noting that $w=w(i_p,r_A)$ and $n_r=nr(i_p,\varepsilon_p/\varepsilon_t)$. A detailed description of the pore-wall roughness model is reported by Tsakiroglou and Payatakes (1993).

2.2 Calculation of absolute permeability and formation factor

The calculation of the formation factor of pore-and-throat networks is reduced directly to the analysis of electric circuits, whereas the absolute permeability is calculated by analogy to electric circuits. The pressure, the hydraulic conductance and the volumetric flow rate are equivalent to the potential, the electrical conductance and the current flow. Kirchoff's rules formulate that the sum of the voltages is zero for every closed loop of conductors and that the algebraic sum of the currents flowing into each node is also zero. From the application of these rules to the pore network, a system of coupled linear equations for the potential at each

node is obtained. This system is solved using an iterative Gauss-Seidel method. Substituting the volumetric flow rate at the inlet of network and the pressure drop along it in Darcy's law, the absolute permeability is obtained. Each unit cell consists of a throat and two hemispherical pores. For the sake of simplicity, each spherical segment of a unit cell is replaced by a cylindrical one, having diameter equal to the average of the throat and pore diameters. The fractal roughness features of throats and pores are included in the calculation of hydraulic and electrical conductances by regarding them as cylindrical shells the thickness of which is decided by the total roughness volume.

3. SIMULATION OF DRAINAGE AND IMBIBITION

Drainage is a process where a non-wetting fluid displaces a wetting one at increasing values of the capillary pressure, whereas the reverse process is defined as imbibition The contact angle measured with respect to aqueous phase (brine), θ, is used to quantify the wettability of a pore network. If $\theta \le \pi/2$ then the pore network is defined as water-wet, and if $\theta > \pi/2$ the pore network is defined as oil-wet. In a water-wet case, initially the pore network is occupied by brine (aqueous solution of an electrolyte) which is gradually displaced by oil. In contrast, in an oil-wet case the defender is oil and the invader is brine.

3.1 Drainage in water-wet networks

At a current value of the capillary pressure, the pore network is scanned to search of throats that are accessible to the external oil sink and have size that allows a meniscus to penetrate into them. As soon as a throat is filled with oil, the adjoining water-occupied pores are invaded by oil spontaneously. The procedure is repeated until no more meniscus moves, and capillary equilibrium is established. Then a pressure difference is imposed across the network, the Kirchoff's rules are applied separately to the equivalent electric sub-network of each phase. From the numerical solution of the resulting system of linear equations, the pressure at the centre of each pore and the flow rate of the wetting and non-wetting phases at each unit cell are calculated, and used in the Darcy law for two-phase flow to determine the water and oil relative permeability. Likewise a voltage is imposed across the network, and the calculated electrical current intensities at each unit cell are used in Ohm's law to calculate the electrical resistivity index defined by

$$I_R = \frac{R(S_w)}{R(S_w = 1)} \tag{1}$$

where $R(S_w)$ is the resistance of the network at water saturation S_w.

Additional assumptions that are adopted to simulate drainage in water-wet networks are summarized below.

(a) Water drains from a throat or pore only if there is a non-interrupted column of water connecting it to the external water sink.
(b) Water remaining along pore-wall roughness can drain unlimitedly as long as its hydraulic continuity is preserved.
(c) Occasionally, blobs of trapped water may be created after the filling of a pore with oil.

(d) The pore network becomes hydraulically conductive to oil after the breakthrough pressure, when a network spanning cluster of oil-occupied pores and throats is created for a first time.
(e) The analytic solution of the problem of the simultaneous flow of two immiscible fluids through a cylindrical tube is employed to calculate the hydraulic conductance of oil and water in throats and pores that are occupied by both fluids. The equivalent hydraulic diameters are determined from the volume fractions of the two phases.
(f) If $\theta \geq \pi/2 - w$, then the shape of an oil/water interface in the interior of a roughness feature is concave, the mean curvature of capillary equilibrium becomes negative, and hence all roughness features are filled spontaneously with oil because of capillary instability. Under such conditions neither pores and throats occupied by trapped blobs of water, nor oil-occupied pores and throats contribute to the electrical and hydraulic conductivity of water

3.2 Drainage in oil-wet networks

An analogous approach based on similar assumptions is used to simulate drainage in an oil-wet network. The most important differences are outlined below.

(a) The network becomes electrically conductive at the breakthrough pressure of the non-wetting fluid (water), and the resistivity index starts to be calculated from this point and on.
(b) The electrical resistance of a pore or throat that is occupied by oil is infinity.
(c) The electrical and hydraulic conductance of pores and throats, occupied by both fluids, are calculated by the aforementioned approach of the two-phase flow in a capillary tube, by simply interchanging the spatial arrangement of the two fluids.
(d) If $\theta \leq \pi/2 + w$ the roughness features are occupied completely by water, otherwise oil films are left around invading water.

3.3 Simulation of imbibition

After the end of a drainage run, the saturation of the wetting fluid has reached its irreducible value, S_{ir}. As the capillary pressure starts decreasing, the wetting fluid (water or oil) may imbibe pores of progressively larger size depending on their accessibility properties. However, it is well-known from earlier experimental and theoretical studies (Tsakiroglou and Payatakes, 1990; Tsakiroglou et al., 1997) that at sufficiently low capillary pressures, thin films of wetting fluid surrounding the non-wetting fluid may collapse in narrow throats, because of capillary instability by a mechanism that called “snap-off”. The critical capillary pressure for snap-off depends on contact angle, and throat geometry (Tsakiroglou et al., 1997). On the one hand, snap-off in throats creates new interfaces that increase the accessibility of the wetting fluid to pores occupied by the non-wetting fluid. On the other hand, frequent snap-off events may lead to the loss of the continuity of the non-wetting fluid so that the residual saturation value, S_r, increases substantially. The pore-level events that are taken into account in the simulation of imbibition are outlined below

(a) The wetting fluid may imbibe a throat that is occupied by the non-wetting fluid through one of the following events:

(i) piston-type displacement, if a meniscus exists at one of the throat ends, the non-wetting fluid is accessible to the external sink, and the capillary pressure is lower than the critical value given by Washburn equation,

(ii) snap-off, when the non-wetting fluid is accessible to the external sink, and is surrounded by a thick film of wetting fluid occupying the pore-wall roughness, whereas the capillary pressure is lower than the critical value for snap-off.

(b) Wetting fluid may imbibe a pore if at least one meniscus exists at one junction of the pore with adjacent throats (which means that at least one of the adjoining throats is occupied by wetting fluid) and the capillary pressure is lower than the critical value given by Washburn equation.

4. RESULTS AND DISCUSSION

A pore-and-throat primary network having the skeleton of a regular cubic lattice was constructed by using log-normal pore (PSD) and throat (TSD) diameter distributions (Table 1). After examining the variation of the number of features, n_r, with the total porosity and the angle of sharpness, w, with the surface area ratio, r_A, the parameter values shown in Table 1 were selected. The calculated values of permeability, k=443 mD, and formation factor, F=12.5, are typical for sandstones.

TABLE 1. Parameter values of the pore-and-throat network.

Parameter	Value	Parameter	Value
TSD: $<D_t>$ (μm)	10.0	Total porosity, ε_t	0.20
σ_t (μm)	3.0	Number of features, n_r	20
PSD: $<D_p>$ (μm)	30.0	Surface area ratio, r_A	100
σ_p (μm)	8.0	Angle of sharpness, w (rad)	0.376
Primary porosity, ε_p	0.15	Number of layers, i_p	4

Under water-wet conditions, the critical contact angle $\theta_c = \pi/2 - w$ (=1.19 rad=68.4°) defines a threshold value above which, no water is left in pore-wall roughness and water saturation reaches its irreducible value at relatively low capillary pressures (Fig.1a). For $\theta \geq \theta_c$ the high pressure part of the capillary pressure curve disappears and information concerning the sizes and volumetric percentage of the roughness porosity is lost (Fig.1a). Instead, for $\theta < \theta_c$ information concerning the structure of the secondary porosity is reflected in capillary pressure curve (Fig.1a). On the other hand, the presence of water pockets in pore-wall roughness for $\theta < \theta_c$ is responsible of the relatively low values of resistivity at low water saturations (Fig.1b). The complete filling of pores and throats with oil ($\theta \geq \theta_c$) results in high values of resistivity index and high values of the mean saturation exponent, <n>, which is defined as the negative slope of resistivity index at log-scale averaged over the full range of water saturations (Fig.1b).

The plateau of the oil relative permeability, $k_{ro}(S_w)$, at low water saturations is associated with the small change of the oil hydraulic conductivity as the thickness of the

wetting films, remaining in the pore-wall roughness, is reduced (Fig.2). At decreasing values of the contact angle the thickness of the films remaining in pores or throats after oil invasion decreases so that the plateau gradually shrinks, and disappears entirely when $\theta \geq \theta_c$ (Fig.2). The water relative permeability $k_{ro}(S_w)$ at low water saturations is also due to the presence of films of wetting fluid along roughness features, and as soon as these films disappear ($\theta \geq \theta_c$) the relative permeability decreases dramatically (Fig.2).

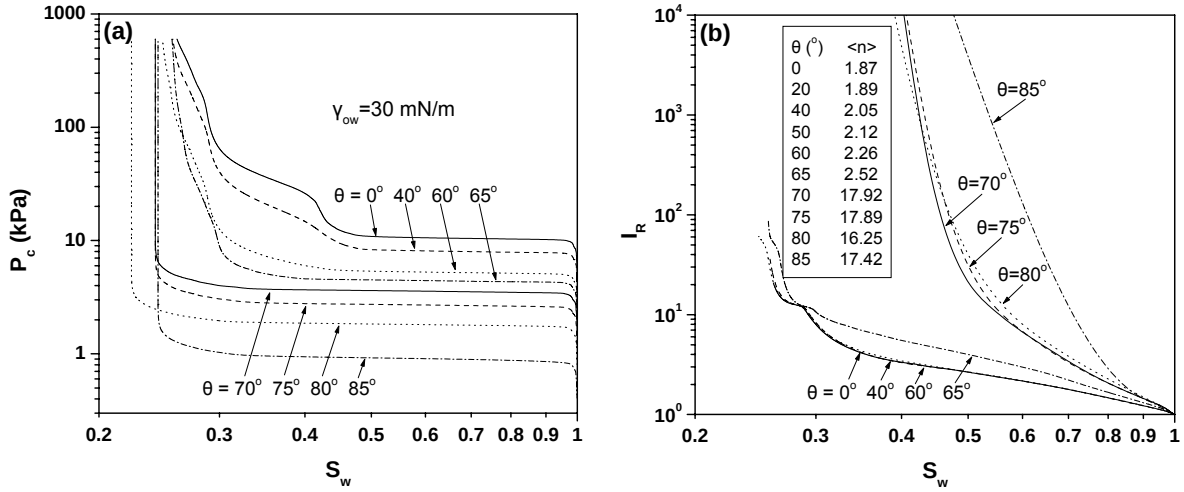

FIGURE 1. Simulated (a) capillary pressure curves and (b) resistivity index curves as functions of the contact angle for drainage in a water-wet pore network

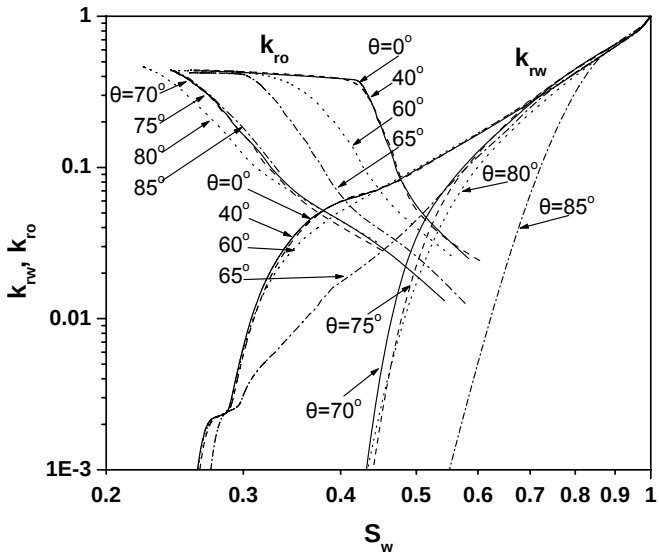

FIGURE 2. Simulated water and oil relative permeability curves as functions of the contact angle for drainage in a water-wet pore network

Secondary imbibition from a water-wet pore network that has been filled under a contact angle 0^o was simulated by using two different approaches: (1) A meniscus moves only if a non-interrupted column of wetting fluid connecting it with the external sink exists, whereas

snap-off in throats does not occur. (2) A meniscus can move independently on its position within the pore network, snap-off may occur, whereas menisci belonging to trapped blobs of oil are excluded from the calculations.

When $\theta \geq \theta_c$, the wetting fluid that has remained in the pore-walls during drainage, is unable to expand at positive values of the capillary pressure with result that imbibition takes place over a narrow pressure range (Figs.3a,4a). It is evident that the inclusion of the snap-off mechanism in the simulations changes drastically the capillary pressure curve over low values of the contact angle (Figs.3a,4a), whereas no important change is caused on the resistivity index curve (Figs.3b,4b).

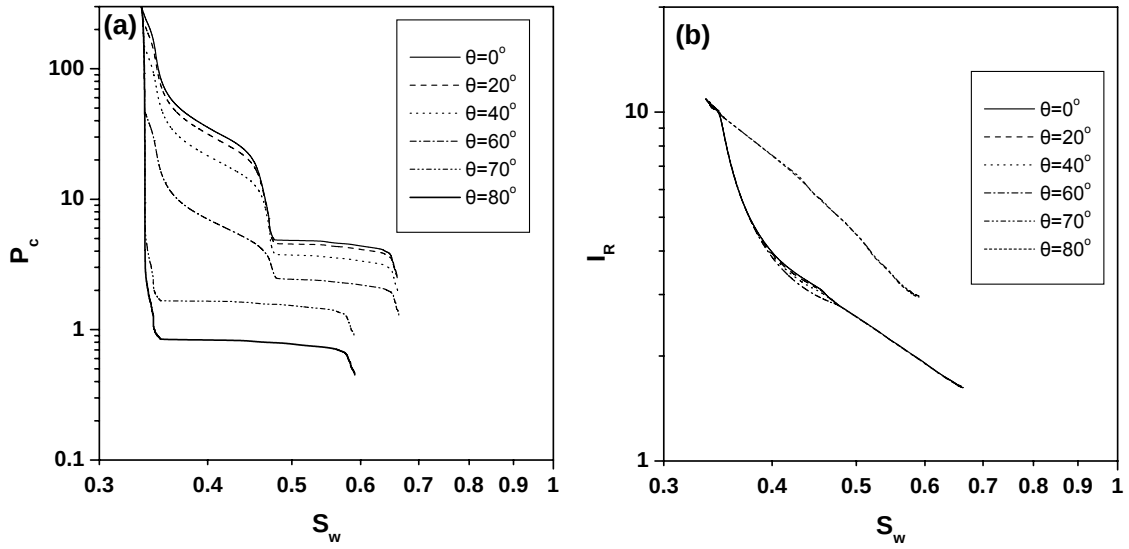

FIGURE 3. Simulated capillary pressure and resistivity index curves as functions of the contact angle for imbibition in a water-wet pore network (without snap-off)

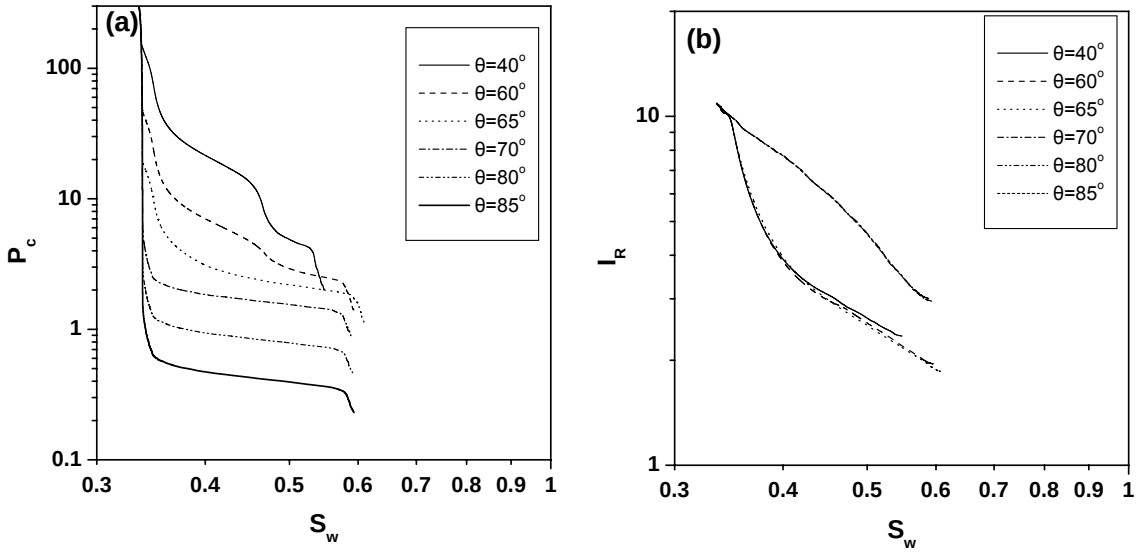

FIGURE 4. Simulated capillary pressure and resistivity index curves as functions of the contact angle for imbibition in a water-wet pore network (with snap-off)

In the present work, mechanistic simulators of oil/water drainage and imbibition in pore-and-throat networks were developed to quantify the capillary, electrical and hydraulic properties of intermediate-wet ($\pi/2 - w \le \theta \le \pi/2 + w$) porous media and give a physical interpretation of the non-linear dependence of the multiphase transport properties on wettability. Moreover, the simulator can be used to correlate explicitly the wettability indices (based on capillary pressure curves) with the relative permeability and resistivity index curves for drainage and imbibition

REFERENCES

1. Anderson, W.G. (1986a), Wettability literature survey-Part 1: rock/oil/brine interactions and the effects of core handling on wettability, *J. Pet. Technol., Oct.*, 1125.
2. Anderson, W.G. (1986b), Wettability literature survey-Part 2: wettability measurement, *J. Pet. Technol. Nov.*, 1246.
3. Blunt, M.J. (1998), Physically based network modeling of multiphase flow in intermediate wet porous media", *J. Pet. Sci. Eng.*, *20*, 117.
4. Bradford, S.A., L.M. Abriola, F.J. Leij (1997), Wettability effects on two – and three fluid relative permeabilities, *J. Contaminant Hydrology, 28*, 171.
5. Dicarlo, D.A., A. Sahni, M. J. Blunt (2000), The effect of wettability on three – phase relative permeability, *Transp. Porous Media, 39*, 347.
6. Dixit, A.B., J.S. Buckley, S.R. McDougall and K.S. Sorbie (2000), Empirical measures of wettability in porous media and the relationships between them derived from pore-scale modeling, *Transp. Porous Media 40*, 27.
7. Dominguez, A., H. Perez-Aguilar, F. Rojas and I. Kornhauser (2001), Mixed wettability: a numerical study of the consequences of porous media morphology, *Colloids and Surfaces A: Phys. & Eng. Aspects, 187-188*, 415.
8. Hazlett, R.D., S.Y Chen, W.E. Soll (1998), Wettability and rate effects on immiscible displacement: Lattice Boltzmann simulation in microtomographic images of reservoir rocks, *J. Pet. Sci. Eng., 20*, 167.
9. Jackson, M.D., P.H. Valvatne, and M.J. Blunt (2003), Prediction of wettability variation and its impact on flow using pore- to reservoir- scale simulations, *J. Pet. Sci. Eng.*, *39*, 231.
10. Kovscek, A.R., H. Wong and C.J. Radke (1993), A pore-level scenario for the development of mixed wettability in oil reservoirs, *AIChE J., 39*, 1072.
11. Laroche, C., O. Vizika, F. Kalaydjian (1999), Network modeling as a tool to predict three-phase gas injection in heterogeneous wettability porous media, *J. Pet. Sci. Eng.*, *24*, 155.
12. Man, H.N., and X. D. Jing (1999), Network modeling and pore geometry effects on electrical resistivity and capillary pressure, *J. Pet. Sci. Eng.* , *24*, 255.
13. Morrow, N.R. (1976), Capillary pressure correlations for uniformly wetted porous media, *J. Can. Pet. Tech. 15,* 49.
14. Morrow, N.R. (1990), Wettability and its effects on oil recovery, *J. Pet. Tech.*, *December*, 1476.
15. Sahimi M. (1995), Flow and Transport in Porous Media and Fractured Rock**:** From Classical Methods to Modern Approaches, VCH, Weinheim, Germany.
16. Tsakiroglou, C.D., and M. Fleury (1999), Resistivity index of fractional wettability porous media, *J. Pet. Sci. Eng.*, *22*, 253.
17. Tsakiroglou, C.D., G.B. Kolonis, T.C. Roumeliotis and A.C. Payatakes (1997), Mercury penetration and snap-off in lenticular pores, *J. Colloid Interface Science*, *193*, 259.
18. Tsakiroglou, C.D. and A.C. Payatakes (1990), A new simulator of mercury porosimetry for the characterization of porous materials, *J. Colloid Interface Sci.*, *137*, 315.
19. Tsakiroglou,C.D., and A.C. Payatakes (1993), Pore-wall roughness as a fractal surface and theoretical simulation of mercury intrusion/retraction in porous media, *J. Colloid Interface Sci.*, *159*, 287.
20. Van Dijke, M.I.J., K.S. Sorbie, and S.R. McDougall (2001), Saturation –dependencies of three-phase relative permeabilities in mixed-wet and fractionally wet systems, *Adv. Water Resour., 24*, 365.